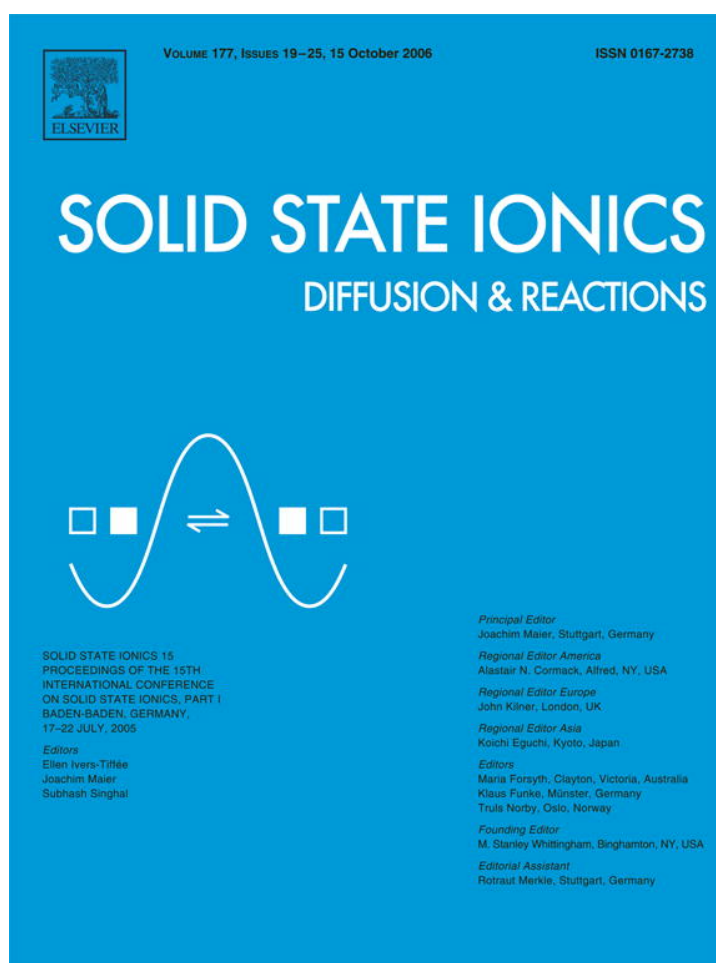


Provided for non-commercial research and educational use only.
Not for reproduction or distribution or commercial use.



This article was originally published in a journal published by Elsevier, and the attached copy is provided by Elsevier for the author's benefit and for the benefit of the author's institution, for non-commercial research and educational use including without limitation use in instruction at your institution, sending it to specific colleagues that you know, and providing a copy to your institution's administrator.

All other uses, reproduction and distribution, including without limitation commercial reprints, selling or licensing copies or access, or posting on open internet sites, your personal or institution's website or repository, are prohibited. For exceptions, permission may be sought for such use through Elsevier's permissions site at:

<http://www.elsevier.com/locate/permissionusematerial>

High temperature properties of the $n=2$ Ruddlesden–Popper phases (La,Sr)₃(Fe,Ni)₂O_{7- δ}

L. Mogni^a, F. Prado^{a,*}, A. Caneiro^a, A. Manthiram^b

^a Centro Atómico Bariloche, CNEA, S. C. de Bariloche 8400, Argentina

^b Materials Science and Engineering Program, The University of Texas at Austin, Austin, TX 78712, USA

Received 6 June 2005; received in revised form 3 February 2006; accepted 29 March 2006

Abstract

The crystal chemistry and mixed conductor properties of the $n=2$ member of the Ruddlesden–Popper (R–P) phases Sr_{3-x}La_xFe_{2-y}Ni_yO_{7- δ} with $0 \leq x \leq 0.3$ and $0 \leq y \leq 1.0$ have been studied at high temperature. High-temperature X-ray diffraction and thermogravimetric measurements of the equilibrium pO_2 ($10^{-5} \leq pO_2 \leq 1$ atm) in the temperature range $400 \leq T \leq 1000$ °C indicate that the Sr₃FeNiO_{7- δ} phase is able to accommodate a large oxygen non-stoichiometry ($\delta \sim 1.5$) without structural transformations. The electrical conductivity and oxygen permeability increase with the substitution of Ni for Fe in the range $550 \leq T \leq 1000$ °C. The electrical transport of the Sr₃FeNiO_{7- δ} phase is thermally activated and the activation energy decreases with the substitution of Ni for Fe for a given oxygen content. The increase in the oxygen permeation flux with increasing Ni content is due to an increasing oxygen non-stoichiometry and a lower activation energy for permeation.

© 2006 Elsevier B.V. All rights reserved.

Keywords: Mixed conductors; Ruddlesden–Popper phases; Oxygen non-stoichiometry; Electrical conductivity; Oxygen permeation

1. Introduction

With an aim to develop mixed conducting oxides that are chemically and structurally more stable than the conventional perovskite phases La_{1-x}Sr_xFe_{1-y}Co_yO_{3- δ} , perovskite-related intergrowth structures have drawn interest recently [1–3]. The Ruddlesden–Popper (R–P) series Sr _{$n+1$} Fe _{n} O_{3 $n+1$} belong to this class of materials, and it consists of n blocks of SrFeO₃ perovskite layers alternating with SrO rock salt layers along the c axis [4]. The $n=2$ member of the R–P series, Sr₃Fe₂O_{7- δ} , has a crystal structure with tetragonal symmetry (S. G. I4/mmm) isostructural with Sr₃Ti₂O₇ [4]. Recently, the crystal chemistry and mixed conducting properties of Sr₃Fe₂O_{7- δ} and the solid solution Sr_{3-x}La_xFe_{2-y}Co_yO_{7- δ} have been studied for $0 \leq x \leq 0.3$ and $0 \leq y \leq 1.0$ [2,5]. The parent compound Sr₃Fe₂O_{7- δ} exhibits a large oxygen non-stoichiometry, $\delta \sim 1.0$ at $T=1000$ °C and $pO_2 \sim 10^{-5}$ atm [6], which increases up to $\delta=1.5$ for the Co-doped sample with $y=1.0$ [7]. More interestingly, the crystal structure tolerates the large oxygen

non-stoichiometry values without any change in the symmetry [6,7]. Following this trend, it is expected that the partial substitution of Ni for Fe will also lead to high oxygen non-stoichiometry values due to the difficulty of stabilizing the Ni^{3+/4+} oxidation state compared to that of Fe^{3+/4+}, improving the oxide-ion conductivity of the Sr₃Fe₂O_{7- δ} phase. Recently, we reported the physical properties at low temperatures of the system Sr₃Fe_{2-y}Ni_yO_{7- δ} with $0 \leq y \leq 1.0$. It was found that the substitution of Ni for Fe improves the electrical conductivity of the Sr₃Fe₂O_{7- δ} phase at low temperature mainly due to a reduction of the p - d transfer integral value [8]. We present here the crystal chemistry and mixed conductor properties at high temperature of the system (La,Sr)₃(Fe,Ni)₂O_{7- δ} by investigating the structural stability, oxygen non-stoichiometry, and electrical conductivity as a function of oxygen content and oxygen permeability.

2. Experimental

The (La,Sr)₃(Fe,Ni)₂O_{7- δ} samples were prepared by an acetic acid-based gel route using SrCO₃ (99.99%), La₂O₃ (99.99%), Fe(CH₃COO)₂ (99%), and Ni(CH₃COO)₂·3H₂O

* Corresponding author. Fax: +54 2944 445299.

E-mail address: fprado@cab.cnea.gov.ar (F. Prado).

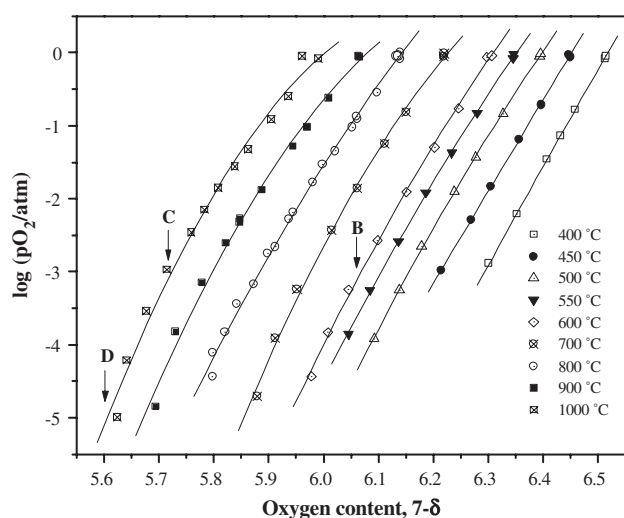


Fig. 1. Log(pO_2) vs. oxygen content curves at various temperatures of $Sr_3FeNiO_{7-\delta}$. Points B, C, and D indicate the T and pO_2 conditions of the XRD data displayed in Fig. 2 at $T > 20$ °C.

(99%+) as raw materials following the procedure described elsewhere [8]. The final heat treatment was carried out at 1300 °C under flowing oxygen for a period of 24 h. The formation of single-phase materials was verified by X-ray diffraction (Philips PW1700 diffractometer) using Cu $K\alpha$ radiation and graphite monochromator. Thermogravimetric and electrical conductivity measurements were performed on the $Sr_3Fe_2O_7$ and $Sr_3FeNiO_{7-\delta}$ phases. Oxygen permeation measurements were carried out on $La_{0.3}Sr_{2.7}Fe_{2-y}Ni_yO_{7-\delta}$ samples. The substitution of La for Sr was found to be beneficial in suppressing the structural and chemical instabilities and reactivity at room temperature of the La-free compounds.

High-temperature X-ray diffraction data were collected by spreading the sample onto a resistively heated platinum ribbon in an Anton Paar HTK-10 chamber coupled to the diffractometer. Thermogravimetric measurements were performed with a symmetrical thermobalance based on a Cahn 1000 electrobalance. Equilibrium pO_2 measurements were carried out with the thermobalance coupled to an electrochemical system for the measurement and control of pO_2 [9]. The equilibrium for a given T and pO_2 is defined as a condition in which the sample weight remains constant within 10 μg over a period of 24 h. The absolute oxygen content $y=f(T, pO_2)$ of each equilibrium point was obtained after reducing the sample in a mixture of 90% Ar and 10% H_2 at 1100 °C and assuming SrO, Fe, and Ni as the reduction products. The reduction of the samples was carried out after the corresponding equilibrium pO_2 measurements were finished. DC resistivity measurements at high temperature and controlled pO_2 were carried out by a standard four-probe method on bar shaped, dense samples. Oxygen permeation measurements were carried out with sintered, polished discs having a thickness of about 1.5 mm and densities >90% of the theoretical density; it involved the exposure of one side of the disc to air (pO_2) and the other side to a lower oxygen partial pressure (pO_2') controlled by flowing He. The oxygen flux

across the membranes was evaluated employing a HP 5880A gas chromatograph [1–3].

3. Results and discussion

The crystal structures of the $Sr_{3-x}La_xFe_{2-y}Ni_yO_{7-\delta}$ compounds with $x=0$ and 0.3 and $y=0$ and 1.0 were refined based on the tetragonal space group I4/mmm [4] using the X-ray powder diffraction data collected at room temperature. The crystal structure symmetry does not change on substituting La^{3+} for Sr^{2+} and Ni^{3+} for $Fe^{3+/4+}$. The lattice parameters a and c and the unit cell volume V decrease with increasing Ni content [8] due to a smaller ionic radii of Ni^{3+} and Ni^{4+} compared to those of Fe^{3+} and Fe^{4+} [10]. No secondary phases were detected by X-ray diffraction.

Fig. 1 shows the variation of the oxygen content as a function of the equilibrium pO_2 ($10^{-5} \leq pO_2 \leq 1$ atm) of the $Sr_3FeNiO_{7-\delta}$ phase for various temperatures in the range $400 \leq T \leq 1000$ °C. The log(pO_2) vs. oxygen content curves for $Sr_3FeNiO_{7-\delta}$ reveal a large field of oxygen non-stoichiometry ($1.4 \leq \delta \leq 0$) for this material with no evidence of the formation of a stable compound with an average oxidation state +3 at $\delta=1.0$ as was observed for $Sr_3Fe_2O_{7-\delta}$ [6]. Although thermogravimetric measurements do not suggest any structural transformation, the crystal structure stability was further studied by means of high temperature X-ray diffraction measurements under controlled

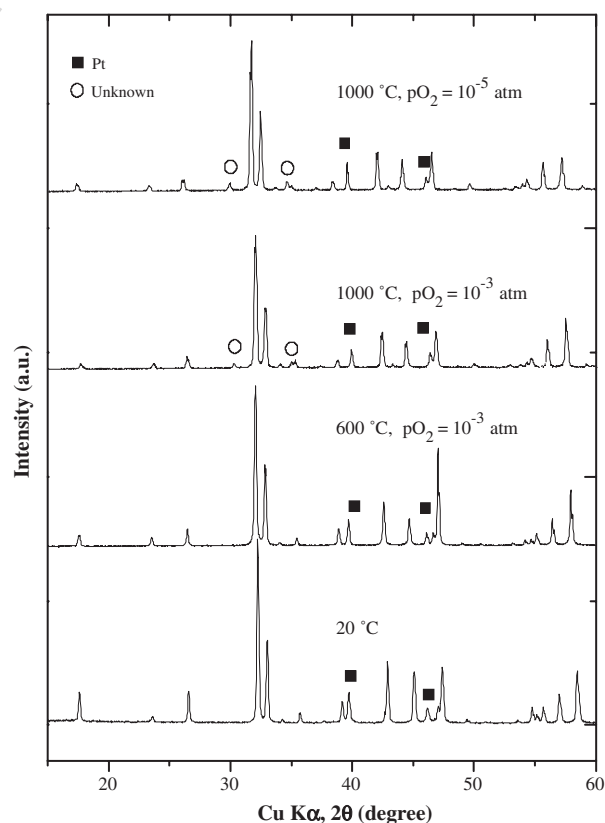


Fig. 2. X-ray diffraction patterns of $Sr_3FeNiO_{7-\delta}$ at (a) room temperature, (b) 600 °C, and (c) 1000 °C under $pO_2=10^{-3}$ atm, and at (d) 1000 °C under $pO_2=10^{-5}$ atm.

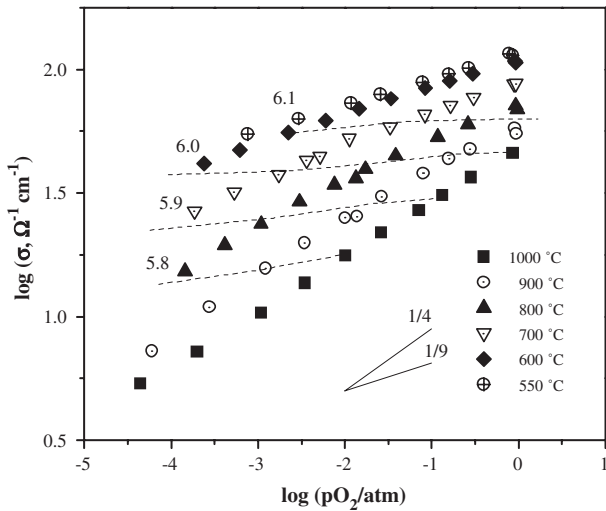


Fig. 3. Log(σ) vs. log(pO_2) curves of $Sr_3FeNiO_{7-\delta}$ at various temperatures. The dashed lines indicate log(σ) vs. log(pO_2) data at a constant oxygen content.

atmosphere. Fig. 2 compares the X-ray data of the $Sr_3FeNiO_{7-\delta}$ phase obtained at $T=20$, 600, and 1000 °C under $pO_2=10^{-3}$ atm and $T=1000$ °C under $pO_2=10^{-5}$ atm. The values of T and pO_2 used for the XRD at high temperatures are marked with letters in Fig. 1. The XRD data confirm that $Sr_3FeNiO_{7-\delta}$ phase is able to accommodate a high concentration ($\sim 20\%$) of oxygen vacancies without any change in the crystal structure in the whole range of T and pO_2 explored in this study. This behavior is similar to that found before for the Co-doped compound $Sr_3FeCoO_{7-\delta}$ [7]. The appearance of weak, extra peaks at 1000 °C in Fig. 2 is related to the chemical reaction of $Sr_3FeNiO_{7-\delta}$ with the Pt ribbon of the high temperature camera.

The variation of the electrical conductivity as a function of T and equilibrium pO_2 of $Sr_3FeNiO_{7-\delta}$ is shown in Fig. 3. The slope of the log(σ) vs. log(pO_2) isotherms is positive, which indicates the formation of p -type (hole) carriers, and varies from

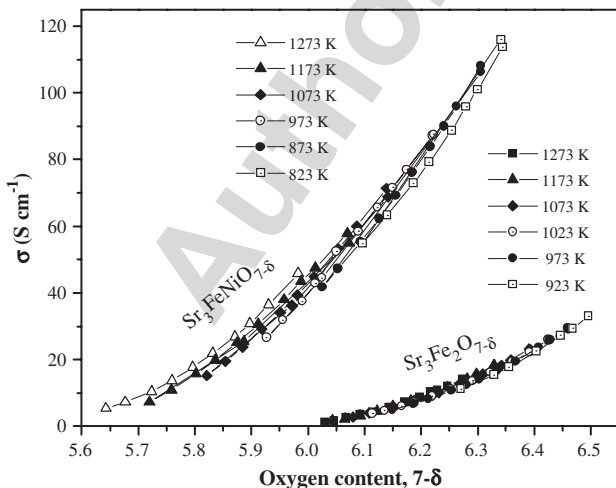


Fig. 4. Variations of σ with the oxygen content at various temperatures for $Sr_3FeBO_{7-\delta}$ (B=Fe and Ni).

$\sim 1/4$ at $T=1000$ °C to $1/9$ at $T=550$ °C. Constant oxygen content lines are included in Fig. 3 on the log(σ) vs. log(pO_2) curves. The log(σ) vs. log(pO_2) data can be roughly divided in two regions by the line $7-\delta=6.0$ that corresponds to the average oxidation state of +3. Thus, the curves have a slope of $\sim 1/4$ for $7-\delta < 6.0$ and $\sim 1/9$ for $7-\delta > 6.0$. The electrical conductivity increases slightly with increasing temperature for a given oxygen content, indicating that the electrical transport process is thermally activated. The activation energy values estimated from the slopes of the log($\sigma T^{3/2}$) vs. $1/T$ curves (small polaron) or log($\sigma T^{1/2}$) vs. $1/T$ curves (large polaron) were ~ 0.16 and 0.05 eV, respectively, in the oxygen content range of $6.0 > 7-\delta > 6.2$. These values are smaller than the value of ~ 0.20 eV obtained for $Sr_3Fe_2O_{7-\delta}$ with the small polaron model for similar oxygen contents [6]. The variations of σ with the oxygen content at various T are shown in Fig. 4. The curves were obtained from the combination of thermogravimetric and electrical conductivity measurements as a function of the equilibrium pO_2 . The electrical conductivity of the $Sr_3FeNiO_{7-\delta}$ sample is almost one order of magnitude higher than that of the $Sr_3Fe_2O_{7-\delta}$ phase for a given oxygen content. The increase in the electrical conductivity with the substitution of Ni for Fe was also observed at low temperatures, and it was attributed to the reduction of the $p-d$ transfer integral [8]. The thermally activated behavior of σ , its evolution with the oxygen content (see Fig. 4), the decrease of the activation energy with increasing the oxygen content (not shown here), indicate that the electrical transport in $Sr_3FeNiO_{7-\delta}$ is consistent with a polaron type behavior. Further analysis is in progress to understand in detail the electrical transport behavior of $Sr_3FeNiO_{7-\delta}$.

Fig. 5 shows the variation of the oxygen permeation flux jO_2 with the inverse temperature of the $La_{0.3}Sr_{2.7}FeMO_{7-\delta}$ (M=Fe, Co and Ni) compounds at a constant pO_2 gradient of log(pO_2/pO_2')=2.2 across the membrane. The substitution of Ni for Fe increases the jO_2 values across the membrane, although they are lower than those reported for a membrane of $La_{0.3}Sr_{2.7}FeCoO_{7-\delta}$ [2]. Activation energy values related to the

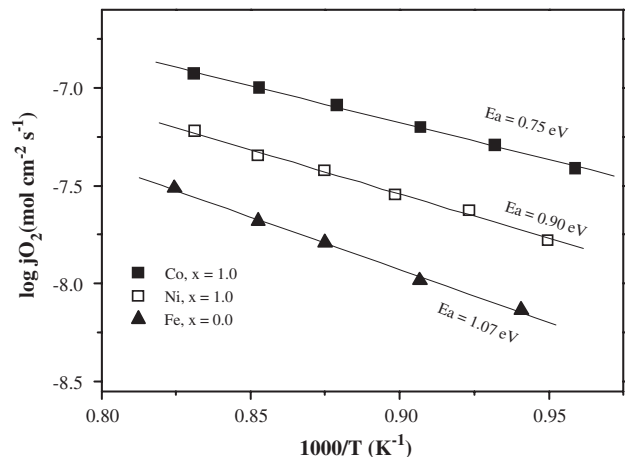


Fig. 5. Arrhenius plot of jO_2 for $Sr_{2.7}La_{0.3}Fe_{2-x}B_xO_{7-\delta}$ (B=Fe, Co and Ni) at a constant log(pO_2/pO_2')=2.2. The membranes were 1.5 mm thick.

oxygen permeation mechanism were computed from the slope of the $\log(jO_2)$ vs. $1/T$ curves. The activation energy decreases with increasing Ni and Co contents, although the minimum activation energy was reported for the $La_{0.3}Sr_{2.7}FeCoO_{7-\delta}$ compound ($E_a=0.75$ eV) [2]. The decrease in the activation energy is consistent with the increase in the oxygen permeation flux with increasing Ni and Co contents. Interestingly, the $n=2$ member ($Sr_3Fe_2O_7$) of the R–P phase allows to study the effects of the partial substitution of the B site on the high temperature properties while the crystal structure symmetry remains the same, unlike most of the $ABO_{3-\delta}$ perovskite oxides. The increase in the oxygen permeation flux values observed in the Ni-containing samples may be associated with the larger values of oxygen non-stoichiometry and the increase in the electrical conductivity on replacing Fe by Ni. This increase, however, is observed while the unit cell volume V decreases, which could reduce the oxide-ion mobility. Similar results were found before on replacing Fe by Co. Thus, the larger permeation rates reported for the Co containing samples [2] compared to the $La_{0.3}Sr_{2.7}FeNiO_{7-\delta}$ compound may be related to a smaller contraction of the unit cell volume, and also to the improvement in the oxygen exchange kinetic at the surface of the membrane due to the presence of Co.

4. Conclusions

The crystal structure of the $n=2$ member of the R–P phases $(La,Sr)_3(Fe,Ni)_2O_{7-\delta}$ remains stable without any phase transformation in the high-temperature range of $400 \leq T \leq 1000$ °C and pO_2 values of $10^{-5} \leq pO_2 \leq 1$ atm. The substitution of Ni for Fe increases the range of oxygen non-stoichiometry up to $\delta \sim 1.5$. Electrical conductivity measurements at high temper-

ature indicate that the charge carriers are electron holes and the electrical transport is thermally activated. The oxygen permeation flux values increase with increasing Ni content as a consequence of the larger oxygen non-stoichiometry that enhances the oxide ion mobility. The jO_2 values of the $(La,Sr)_3(Fe,Ni)_2O_{7-\delta}$ samples are still lower than those obtained for the analogous R–P phases containing Co.

Acknowledgements

This work was supported by CNEA (Argentine Atomic Energy Commission), Fundación Antorchas, ANPCyT through PICT 02-12-12455 and 03-12-14493, Cooperation Program ECOS-SUD, and the Welch Foundation Grant F-1254.

References

- [1] T. Armstrong, F. Prado, Y. Xia, A. Manthiram, J. Electrochem. Soc. 147 (2000) 435.
- [2] F. Prado, T. Armstrong, A. Caneiro, A. Manthiram, J. Electrochem. Soc. 148 (2001) J7.
- [3] T. Armstrong, F. Prado, A. Manthiram, Solid State Ionics 140 (2001) 89.
- [4] S.N. Ruddlesden, P. Popper, Acta Crystallogr. 11 (1958) 54.
- [5] Y.A. Shilova, M.V. Patrakeev, E.B. Mitberg, I.A. Leonidov, V.L. Kozhevnikov, K.R. Poeppelmeier, J. Solid State Chem. 168 (2002) 275.
- [6] L. Mogni, F. Prado, A. Caneiro, J. Fouletier, J. Solid State Chem. 178 (2005) 2715.
- [7] Y. Bréard, C. Michel, M. Hervieu, F. Studer, A. Maignan, B.B. Raveau, Chem. Mater. 14 (2002) 3128.
- [8] L. Mogni, F. Prado, H. Ascolani, M. Abbate, M.S. Moreno, A. Manthiram, A. Caneiro, J. Solid State Chem. 178 (2005) 1559.
- [9] A. Caneiro, P. Bavdaz, J. Fouletier, J.P. Abriata, Rev. Sci. Instrum. 53 (1982) 1072.
- [10] R.D. Shannon, Acta Crystallogr., A 32 (1976) 751.